Journal of Nano- and Electronic Physics
Vol. **12** No 4, 04012(5pp) (2020)

Журнал нано- та електронної фізики
Том **12** № 4, 04012(5cc) (2020)

Structural Studies of Mechanically Alloyed $Fe_{1-x}Al_x$ Powder

S. Khan[1], A. Vyas[1], S. Rajan[2], S. Jani[3], R. Brajpuriya[1,*]

[1] *Amity University Haryana, Manesar, Gurgaon, Haryana, India*
[2] *Department of Applied Sciences and Humanities, Chaudhary Ranbir Singh State Institute of Engineering and Technology, Silani Kesho Jhajjar, Haryana, India*
[3] *Department of Applied Physics, Amity School of Pure and Applied Sciences, Amity University Madhya Pradesh, Gwalior, MP, India*

(Received 24 April 2020; revised manuscript received 15 August 2020; published online 25 August 2020)

A study was made on the identification of change of structure of $Fe_{1-x}Al_x$ alloy samples prepared by ball milling. The XRD, SEM and TEM techniques were used to study the structural and morphological modifications in the samples as a function of x and milling. As a result of milling (5 h), whole bulk of Fe and Al powder is mostly converted into an ordered solid solution. The planes are mostly aligned along (110) direction of Fe and depict a crystalline structure regardless of the value of x. As a result of milling, Fe-rich phases are formed in the case of Fe-rich samples, whereas, Al-rich phases dominate as the Al rich content increases. Similar information was also received from the SEM and TEM studies, showing the complete disappearance of the initial shape and emergence of a structure which is a composite of large and small grains of diverse sizes due to severe fracture and cold welding due to milling. The average grain size of about 6-8 nm was obtained after 5 h of milling using XRD which is also confirmed by SEM and TEM. The process of transition to nanostructured alloy leads to expansion of lattice parameters along with reduction in grain size.

Keywords: FeAl alloy, TEM, Ball milling.

DOI: 10.21272/jnep.12(4).04012

PACS numbers: 71.20.Lp, 81.20.Ev, 87.64.Bx, 8.37.Hk, 68.37.Lp

1. INTRODUCTION

Intermetallic-phase based FeAl and Fe_3Al alloys, also known as iron aluminides, because of their interesting and useful properties including low density, high hardness, good corrosion, oxidation and carbonization resistance, high melting temperature, good strength both at room and elevated temperatures, as well as high reactance at high temperatures, have become the most attracting materials of research and development [1-10]. FeAl alloys have been studied from the past few decades using various techniques due to their advantageous magnetic and structural properties and undeveloped future applications. The Fe to Al atomic content ratio is one of the key components in deciding the type of structure and formation of various phases. It is important to note that when applying a non-equilibrium process such as mechanical alloying (MA), the complex magnetic phases can be obtained. Nano-structuring and disordering accompanied with the presence of intermediate complex phases result in quite interesting magnetic characteristics [11]. Both from the point of view of understanding the collective behavior of the magnetic phases and also possible applications, the study of such intermediate phases is expected to be very rewarding. Therefore, in this paper we have critically examined the structural and morphological transformation of Fe-Al powders mixed in various compositions by ball milling.

2. EXPERIMENTAL DETAILS

The MA technique was employed to prepare an array of $Fe_{1-x}Al_x$ alloy samples in a range $0.3 \le x \le 0.6$ using the analytical grade iron and aluminum powders of 99.9 % purity. The alloy samples were prepared in a non-reactive environment of Ar in a SPEX 8000M high-energy ball mill. The weight ratio of ball to powder was maintained to 20:1. Bruker D-8 Advance X-ray diffractometer with Cu-K_a radiation was employed for microstructural characterization of the milled powder samples. To explore the structural and morphological changes in the ball milled alloyed powder samples, scanning (SEM) and transmission (TEM) electron microscopy methods were employed.

3. RESULTS AND DISCUSSION

3.1 X-ray Diffraction (XRD)

It is necessary to have the information of crystal structure in order to follow phenomena like phase transformation and alloy formation. Therefore, assigning the correct Miller indices to each peak is very important while indexing the pattern. When reflection takes place for unmixed values of hkl (all even or all odd), the lattice is fcc and it is bcc if the reflection occurs from $h + k + l =$ even. Table 1 depicts the crystal structure and Bravais lattice for unmilled $Fe_{0.5}Al_{0.5}$ sample determined from the arrangement of $h^2 + k^2 + l^2$ values in the XRD pattern (see Fig. 1).

Fig. 1 depicts the XRD patterns of elemental Fe and Al powders, unmilled and $Fe_{1-x}Al_x$ powder samples milled for a fixed period of 5 h using ball milling. The elemental Fe and Al powders were also used so that the properties of unmilled and milled FeAl intermetallic alloys could be compared. X-ray diffraction (XRD) pattern of elemental Fe powder shows two reflections corresponding to bcc-Fe (110) at $2\theta = 44.68°$ and bcc-Fe (200)

* ranjeetbjp@yahoo.co.in

at $2\theta = 65.02°$ (Fig. 1). Similarly, elemental Al powder shows the reflections at $2\theta = 38.52°$, 44.63° and 65.02° from fcc-Al (111), (200) (220) planes (Fig. 1). The lattice parameters of elemental Fe and Al powders were also calculated using XRD pattern and were found to be ~ 0.28 nm and ~ 0.41 nm, respectively, and match well with the lattice parameters of elemental Fe and Al.

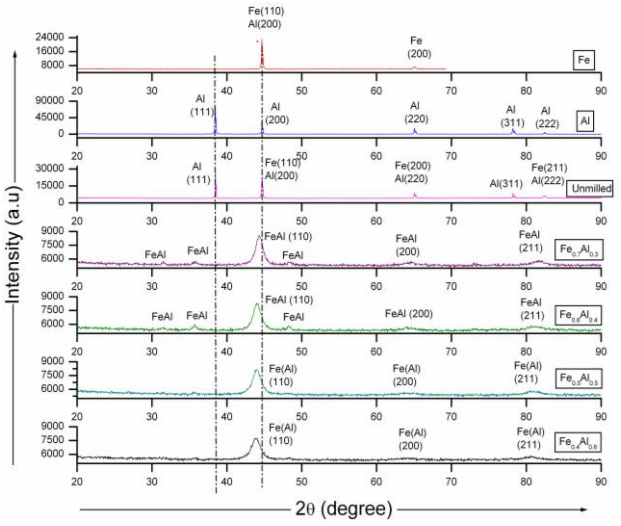

Fig. 1 – XRD patterns of elemental Fe and Al, unmilled and 5 h milled $Fe_{1-x}Al_x$ powders

The XRD pattern of unmilled powder sample shows the peaks corresponding to Fe (bcc) and Al (fcc) metals. This pattern also depicts that the fcc (200) and (220) peaks of Al overlap with the bcc (110) and (200) peaks of Fe and the most intense peak is of Al (111). After milling, however, it is interesting to note that no peaks of starting (unmilled) powder match with any of the peaks of milled samples, clearly indicating the evolution of phase transformation due to milling. The major changes observed after 5 h of milling are: the overall reduction peaks intensity; complete disappearance of the most intense Al (111) peak; the Fe (110) peak intensity increases, and appearance of three new superlattice peaks at $2\theta = 31.56°$, 35.6°, and at 48.24°. The absence of Al peak illustrates the complete dispersal of Al atoms into the lattice of Fe, and together peaks shift towards lower angles and the appearance of superlattice peaks demonstrates the phase evolution from elemental phase to α ordered solid solution of bcc-FeAl. It is also seen from Fig. 1 that the fundamental peaks show consistent broadening and shifting towards lower angles with increment in x.

Peak broadening and shifting of the fundamental peaks is due to the refinement of the crystallite size and an increase in the lattice internal strain in the powder particles, as seen from Table 2. The crystallite size reduces to ~ 8 nm and the lattice parameter (a_0) obtained after milling is found to be greater than that of unmilled Fe indicating lattice expansion. Also, the relative reduction in the integrated intensity (I) of FeAl (110) peak as a function of x (see Table 2) further supports the FeAl alloy formation. The aforementioned effects are assisted by severe plastic deformation and cold welding of elemental Fe and Al powder particles by the impact of balls during ball milling.

Table 1 – Results of the indexing process on unmilled FeAl powder sample

Peak	2θ (°)	$\sin^2\theta$	$\frac{\sin^2\theta}{\sin^2\theta_{min}}$	$h^2+k^2+l^2$	Unmixed (hkl) fcc-Al	$h^2+k^2+l^2$ = even, bcc-Fe
1	38.47	0.19	1	3	111	–
2	44.68	0.14	1.33	4	200	2 (110)
3	65.08	0.29	2.67	8	220	4 (200)
4	78.17	0.40	3.68	11	311	–
5	82.31	0.43	4.00	12	222	6 (211)

It can be further observed that the samples after MA for 5 h duration become crystalline in structure and are mainly textured along (110) direction irrespective of the percentage of Al in it. The peak of high intensity at $2\theta = 44.25°$ position corresponds to FeAl (110), the peaks of lower intensities appearing due to FeAl (110) correspond to FeAl (110), and the other low intensity peaks are due to the reflections from FeAl (100), FeAl (200) and FeAl (211) planes, respectively. It is further interesting to note that along with the FeAl peaks, Fig. 1 also depicts the presence of the superlattice peaks at $2\theta = 31.56°$, 35.6°, and at 48.24°. The presence of these new peaks clearly indicates the precipitation and formation of ordered domains of FeAl solid solution in Fe-rich samples, as these peaks are not present in the diffraction pattern of unmilled powder samples. However, the intensity of these superlattice peaks decreases at higher Al concentrations due to an increase in disorder as a result of diffusion of Al atoms into Fe lattice. The disordering gives rise to expansion in the lattice and the system entropy becomes dominant. The random occupancy of atoms in the bcc FeAl lattice leads to antisite defects and in turn increases the chances of like atoms to be neighbors. In this way, it is possible to hear that an atom occupying a wrong site and the solid solution become thermodynamically metastable as the free energy of Fe (Al) due to the aforementioned phenomenon. In summary, after milling, Fe-rich phases are formed in case of Fe-rich samples, whereas, Al-rich phases dominate as the Al-rich content increases. The Scherrer's equation was used to estimate the average size of the nanoparticles. The average crystallite sizes for milled $Fe_{0.7}Al_{0.3}$, $Fe_{0.6}Al_{0.4}$, $Fe_{0.5}Al_{0.5}$, $Fe_{0.4}Al_{0.6}$ samples are found to be between 8-6 nm, which indicates the saturation of particle size irrespective of Al concentration.

3.2 Scanning Electron Microscopy (SEM)

SEM was used to examine the morphology of the samples. Fig. 2 illustrates the morphology of unmilled powder particles and that of $Fe_{1-x}Al_x$ alloy samples milled for 5 h. For the unmilled powder (Fig. 2a), the existence of iron particles (spherical in shape) and Al particles (irregular lamellar structure) are clearly observed. However, the structure and shape of the particles have been drastically modified due to severe fracture and cold welding of the particles during the mechanical process as indicated from Fig. 2b-f. These figures demonstrate the morphological evolution of $Fe_{1-x}Al_x$ alloys after milling. It can be seen that the initial structure of particles totally disappeared and it became a mixture of

Table 2 – Structural parameters of unmilled and $Fe_{1-x}Al_x$ alloy samples milled for 5 h calculated using XRD

Samples	2θ (°)	*hkl*	bcc/fcc	*d* (nm)	*a* (nm)	*I* (a.u.)	*D* (nm)
Unmilled FeAl	38.47	111	fcc	0.202	0.405	25322	104.2
	44.71	110/200	bcc/ fcc	0.202	0.286	18948	51.7
$Fe_{0.7}Al_{0.3}$	44.29	110/200	bcc/ fcc	0.204	0.288	8533	8.2
$Fe_{0.6}Al_{0.4}$	44.10	110/200	bcc/ fcc	0.205	0.290	3088	7.3
$Fe_{0.5}Al_{0.5}$	44.00	110/200	bcc/ fcc	0.205	0.291	2900	6.4
$Fe_{0.4}Al_{0.6}$	43.89	110/200	bcc/ fcc	0.206	0.292	2455	6.1

particles having different shapes and sizes. After 5 h ball milling, the grain size of elemental Fe and Al particles was reduced to the nanometer scale which provided the strong conditions for the solid-state reaction because Al and Fe particles (constituents) dissolved at the nanograin boundaries. All the above-mentioned changes occurred in the Fe (Al) intermetallic alloys due to forceful impact of the balls during MA which causes plastic deformation, cold welding and fracture of the particles which came in between the colliding balls. As already mentioned before, ball milling is a powerful non-equilibrium processing method capable of producing strengthened alloys and also leads to refinement of the crystallites as continuous fracturing and welding of particles take place due to friction and shock during the ball milling process. The production of finer structure, increase in temperature due to the collision of milling balls, and the diffusion of components at the nanograin boundaries support solid-state reaction to happen.

The growth of particles occurs in five stages which have been identified using SEM micrographs in Fig. 2. The first stage of the evolution is to mix, deform, fracture and weld powder particles which lead to the production of both coarse and fine particles. The welding of the particles dominates during the second stage and the amount of coarse grains increases with a multilayered composite structure. In the third stage, the number of flake-shaped particles decreases abruptly and the formation of composite particles consisting of parallel lamella takes place. In the next stage, the lamella spacing decreases and the structure of the particles changes from linear to complicate because welding of the particles occurs without preference in the orientation of the particles. The fifth stage is typified by refinement of particles size and increase in internal micro-structural homogeneity [5]. The above results are in tune with the XRD results.

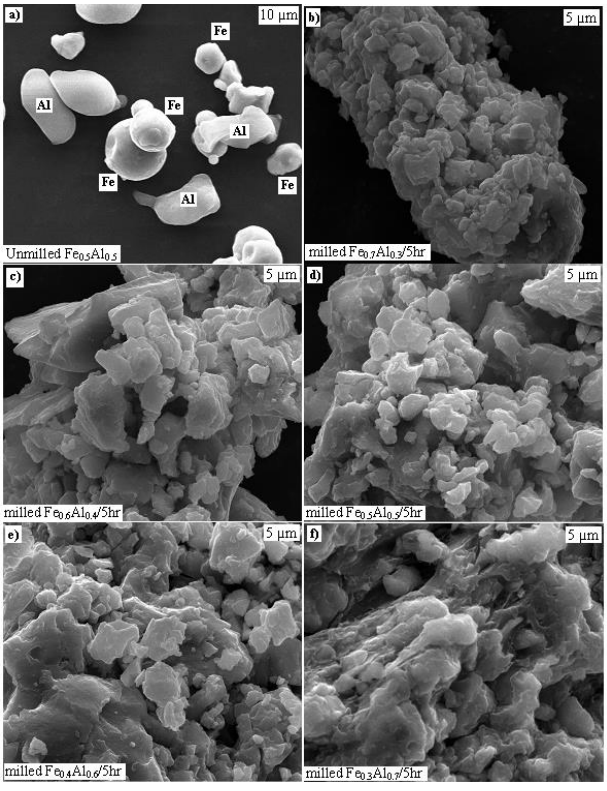

Fig. 2 – SEM images of unmilled and $Fe_{1-x}Al_x$ powders ball milled for 5 h

3.3 Transmission Electron Microscopy (TEM)

TEM bright-field micrographs and electron diffraction patterns of unmilled FeAl and a series of 5 h ball milled $Fe_{1-x}Al_x$ ($0.3 \le x \le 0.6$) intermetallic powder samples are shown in Fig. 3.

Fig. 3a, f depict the electron diffraction pattern and bright-field TEM micrograph of unmilled $Fe_{0.5}Al_{0.5}$ alloy. All the diffraction rings of unmilled $Fe_{0.5}Al_{0.5}$ alloy have been indexed either by fcc-Al and bcc-Fe. The diffraction rings corresponding to Al (111), Al (200), Al (311) and Fe (110), Fe (200), Fe (211) can be clearly seen in Fig. 3a and the diffraction patterns corresponding to Al (200), Al (220) and Al (222) superimpose with Fe (110), Fe (200) and Fe (211) planes. The contrast in TEM micrograph (Fig. 3b) is clearly visible due to the difference in atomic numbers (z) of Fe and Al. The contribution of Al regions will be more than that of Fe regions as Al ($z = 13$) has much smaller electron scattering form factor than Fe ($z = 26$), and therefore the Al crystallites look brighter than Fe crystallites. But after 5 h of milling, the structure and shape of the particles have been changed remarkably. Moreover, some parallel array of fringes is also seen due to the occurrence of plastic deformation during ball milling and powder particles have great agglomeration as welding of particles is introduced during mechanical alloying as shown in Fig. 3. The electron diffraction ring of Al (111) disappears completely, irrespective of Al concentration because of complete disintegration of Al atoms into bcc-Fe lattice which indicates the formation of Fe (Al) solid solution. The decrease in the intensity and broadening of higher order rings are also observed in Fig. 3, which suggests the refinement of the crystallite size and amorphization during mechanical alloying. Moreover, the diffraction rings of Fe are shifted towards the center that further indicates the formation of Fe (Al) solid solution.

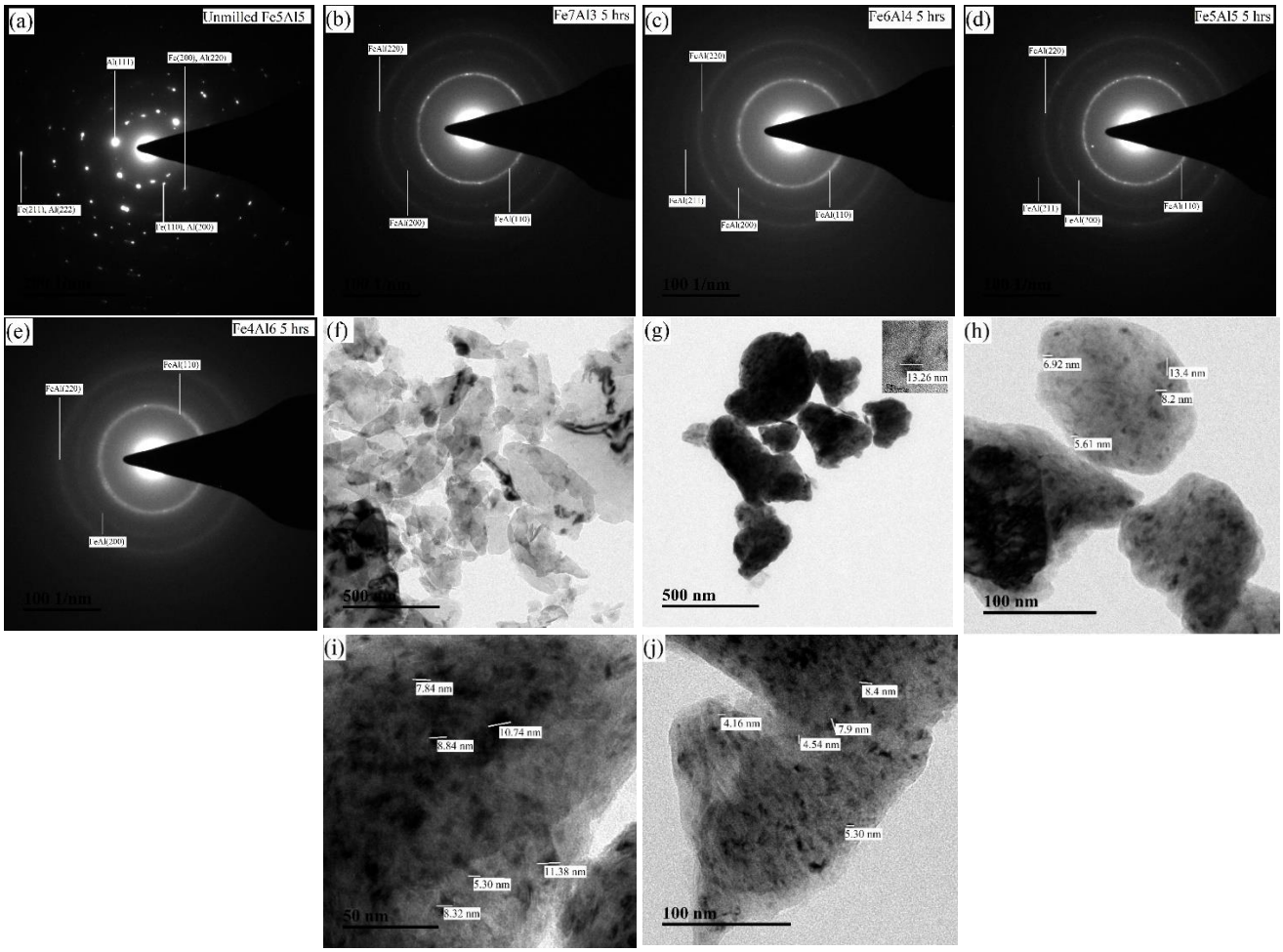

Fig. 3 – The electron diffraction patterns and bright-field TEM images of unmilled and $Fe_{1-x}Al_x$ powders ball milled for 5 h

The bright-field TEM micrographs are used to measure the average crystallite size of powder particles. The diameter of a nanoparticle is measured by averaging its diameters, which are calculated in various directions in the TEM images. The crystallite size of unmilled Fe (Al) alloys measured using TEM is come out to be less than 100 nm, about 62 nm, which is quite consistent with the crystallite size measured using XRD (51.7 nm). However, the average crystallite size of all the Fe (Al) milled samples decreases intensely as compared to unmilled Fe (Al) sample as indicated in Table 3. The average crystallite sizes of 5 h milled $Fe_{0.7}Al_{0.3}$, $Fe_{0.6}Al_{0.4}$, $Fe_{0.5}Al_{0.5}$, $Fe_{0.4}Al_{0.6}$ are found to be 13.2 nm, 8.5 nm, 6.7 nm and 6.1 nm, respectively, that are also in good agreement with the average crystallite sizes measured by XRD. The above-mentioned changes occur due to continuous accumulation and interaction of dislocations which lead to the refinement of crystallite size and increase in the lattice internal strain in the powder particles.

Table 3 – Comparison of crystallite sizes of unmilled and milled samples measured using XRD and TEM

Analysis method	Unmilled	$Fe_{0.7}Al_{0.3}$	$Fe_{0.6}Al_{0.4}$	$Fe_{0.5}Al_{0.5}$	$Fe_{0.4}Al_{0.6}$
XRD '*D*' (nm)	51.7	8.2	7.3	6.4	6.1
TEM '*D*' (nm)	62	13.2	8.5	6.7	6.1

4. CONCLUSIONS

$Fe_{1-x}Al_x$ alloy samples were synthesized and their structural and morphological properties were examined here with respect to change in x. It could be seen here that the process of MA leads to solid-state reaction facilitated by two of the important steps namely severe plastic deformation and cold welding, as a result of which the grain size got reduced and the interesting structural changes developed in the system. There is one thing common in all the compositions, i.e. the disintegration of Al atoms in to the Fe lattice results in the evolution of bcc Fe (Al) solid solution. The texturing was mainly along (110) direction and all the samples were crystalline in nature. Not only the XRD analysis, but SEM and TEM analysis also confirms the process of alloying of elemental powders along with the transition to nanostructured alloy after 5 h of milling. XRD, SEM and TEM results show consistency in results in relation to particle size, phase transformation, and contamination. This system can be suitably studied for magnetization and so as to perceive the type of involved exchange interactions.

ACKNOWLEDGEMENTS

The work has been supported by MPCST for research grant.

REFERENCES

1. S.C. Deevi, V.K. Sikka, *Intermetallics* **4**, 357 (1996).
2. H.D. Guo, Y. Ouyang, *J. Alloy. Compd.* **455**, 207 (2008).
3. W. Hu, T. Kato, M. Fukumoto, *Mater. Transaction* **44**, 2678 (2003).
4. Y.B. Pithawalla, M.S. El Shall, S.C. Deevi, *Intermetallics* **8**, 1225 (2000).
5. S. Rajan, R. Shukla, A. Kumar, A. Vyas, R. Brajpuriya, *Int. J. Mater. Res.* **106**, 114 (2015).
6. C. Gammer, C. Mangler, H.P. Karnthales, C. Rentenberger, *Scripta Mater.* **65**, 57 (2011).
7. Mohsen Mhadhbi, Joan Josep Suñol, Mohamed Khitouni, *Phys. Procedia* **40**, 38 (2013).
8. M. Krashowski, A. Grabias, T. Kulik, *J. Alloy. Compd.* **424**, 119 (2006).
9. Q. Zeng, I. Baker, *Intermetallics* **14**, 396 (2006).
10. U.R. Kattner, *Binary Alloy Phase Diagrams*, *2nd edition, T.B. Massalski, ASM International, Materials Park, OH*, 147 (1990).
11. Z. Hamlati, A. Guittourm, S. Bergheul, N. Souami, K. Taibi, M. Azzaz, *J. Mater. Eng. Performance* **21**, 1943 (2012).

Структурні дослідження механічно легованого порошку $Fe_{1-x}Al_x$

S. Khan[1], A. Vyas[1], S. Rajan[2], S. Jani[3], R. Brajpuriya[1]

[1] *Amity University Haryana, Manesar, Gurgaon, Haryana, India*
[2] *Department of Applied Sciences and Humanities, Chaudhary Ranbir Singh State Institute of Engineering and Technology, Silani Kesho Jhajjar, Haryana, India*
[3] *Department of Applied Physics, Amity School of Pure and Applied Sciences, Amity University Madhya Pradesh, Gwalior, MP, India*

Було проведено дослідження щодо виявлення змін в структурі зразків сплавів $Fe_{1-x}Al_x$, підготовлених методом кульового подрібнення. Методи XRD, SEM і TEM були використані для вивчення структурних та морфологічних модифікацій у зразках як функції x та подрібнення. В результаті подрібнення (5 год) вся маса порошку Fe і Al в основному перетворюється в упорядкований твердий розчин. Площини здебільшого орієнтовані вздовж напрямку Fe (110) і мають кристалічну структуру незалежно від значення x. В результаті подрібнення утворюються фази, збагачені Fe, у випадку зразків, збагачених Fe, тоді як фази, збагачені Al, домінують зі збільшенням вмісту Al. Аналогічна інформація була отримана також у дослідженнях SEM та TEM, які показують повне зникнення початкової форми та появу структури, яка складається з великих та дрібних зерен різного розміру через сильне руйнування та холодне зварювання внаслідок подрібнення. Середній розмір зерна близько 6-8 нм був отриманий після 5 годинного подрібнення з використанням XRD, що також підтверджено дослідженнями SEM і TEM. Процес переходу в наноструктурований сплав призводить до збільшення параметрів решітки разом із зменшенням розміру зерна.

Ключові слова: Сплав FeAl, TEM, Кульове подрібнення.